Potential of hyperspectral imagery for nitrogen content retrieval in sugar beet leaves

S. Jay, X. Hadoux, N. Gorretta, Gilles Rabatel

International Conference of Agricultural Engineering
AgEng 2014 Zurich 6–10 July

Ref: C0357

Potential of hyperspectral imagery for nitrogen content retrieval in sugar beet leaves

Sylvain Jay, Xavier Hadoux, Nathalie Gorretta and Gilles Rabatel, Irstea, 361 rue JF Breton, 34196 Montpellier, France

Abstract

Leaf nitrogen content (LNC) is one of the most important limiting key nutrients in sugar beet crops, so plant nitrogen status has to be carefully monitored throughout the plant life. In this study, close-range hyperspectral imaging was used to infer LNC from reflectance spectra in a non-destructive way and under in-field conditions.
First, after acquisition, images were preprocessed in order to remove some sources of variability that were not correlated to LNC, such as specular reflection and spectral noise. For every hyperspectral image, the mean leaf spectrum was then evaluated and associated to the actual average LNC value measured on the same plants. Partial Least Square regression was used to calibrate a regression model.
With six latent variables, LNC was accurately predicted with a low error and a high coefficient of determination (RMSECV = 1.72 g/kg; R^2 = 0.86). When applied to individual spectra of hyperspectral images, this model led to a consistent LNC map of sugar beet leaves, i.e., LNC was low in old nitrogen-deficient leaves and it was high in young wide leaves. Such a mapping is therefore a valuable non-destructive evaluation tool to better understand how LNC is distributed within plants and to identify LNC-deficient zones.

Keywords: Hyperspectral, leaf nitrogen content, remote sensing, sugar beet.

1. Introduction

Over the last few years, sugar beet (*Beta Vulgaris* L.) has received much attention either for sugar or biofuel productions. It is a credible alternative to sugarcane and therefore, increasing crop yield by creating new varieties consuming less water, pesticides or nitrogen, is currently investigated. Variety selection requires a deep understanding of interactions between genotypes and phenotypes, i.e., how the genes express themselves in a given environment. In particular, how plants assimilate nitrogen, one of the most important limiting key nutrients, is of primary importance and has to be deeply understood in order to optimize nitrogen use.
Phenotypes must be characterized over time and therefore, non-destructive techniques have to be developed. To do so, using leaf optical properties has proven to be a powerful way to infer leaf nitrogen content (LNC), since the latter may strongly affect the leaf spectral transmittance, absorbance and reflectance through the leaf absorption. Usually, LNC is retrieved either by using regression on spectral indices (Wang, et al., 2012) or chemometrics tools such as Partial Least Square regression (PLS) (Vigneau, Ecarnot, Rabatel, & Roumet, 2011).
In this study, we used hyperspectral (HS) imaging because it combines spectral and spatial information into a single multivariate image, thus allowing both the LNC retrieval and LNC mapping within the imaged plants.

Section 2 describes the data acquisition and methods that were used to infer LNC, while Section 3 presents the prediction results and estimated LNC map.

2. Materials and methods

2.1. Data acquisition

HS images were acquired in sugar beet fields in Vimy (northern France) within the framework of AKER project (see Acknowledgements). Two sugar beet varieties (Python and Eleonora) submitted to four different nitrogen fertilizations were studied at two growth stages in June and July 2013. For each of these sixteen combinations, three rows were considered (i.e., 48 combinations), and about five successive plants per row were imaged.
To do so, we used the Becam phenotyping platform presented in Fig. 1. A Hyspex push-broom hyperspectral camera (Norsk Elektro Optikk, Norway) was set up on a translation stage at one meter above the crop row, and was facing towards nadir as seen in Fig. 1b. It acquired successive lines of 1600 pixels and 160 spectral bands ranging from 410 to 1000 nm with a 3.7 nm spectral sampling interval. As the acquired radiance images depended on lighting conditions, they were converted into reflectance images by using the procedure described by Vigneau, Ecarnot, Rabatel, & Roumet (2011), i.e., by introducing a gray reference plate into the scene as observed in Fig. 1.b.

(a) (b)

Figure 1: Becam phenotyping platform: (a) Overall setup, and (b) Hyperspectral camera mounted on the translation stage.

For each crop row, after image acquisition, the limbs of imaged plants were harvested and sent to the laboratory for destructive measurements. The mean LNC of these five plants was then measured using the Kjeldahl method. The LNC ranges (expressed in g/kg dry matter) for the two varieties are reported in Table 1. Note that one sample was discarded because of mishandling. The overall data set was finally made of 47 samples, i.e., 47 images and LNC measurements.

Table 1: Leaf nitrogen content measurements (in g/kg dry matter).

Data set	Number of samples	Min	Max	Mean	Standard deviation
Python	24	34.08	49.64	42.82	5.18
Eleonora	23	37.14	50.12	43.94	4.10
Total	47	34.08	50.12	43.36	4.66

2.2. Spectral preprocessing and PLS model calibration

The spectral information acquired by the HS camera and converted into reflectance could not be directly used to infer LNC. A number of biochemical and geometrical considerations had to be carefully taken into account so that the remaining spectral variability was mainly due to the LNC variability.
Firstly, LNC is often retrieved through the chlorophyll influence, both variables being usually correlated (Schlemmer, et al., 2013). Indeed, Curran (1989) has reported that nitrogen does not absorb light between 400 and 1000 nm, while chlorophyll-a and chlorophyll-b do (at 430 and 460 nm for chlorophyll-a, and at 640 and 660 nm for chlorophyll-b). Moreover, the magnitude of the near-infrared plateau weakly depends on chlorophyll and nitrogen, so in order to remove any variability not strongly related to LNC, the regression model was built using only the 400-700 nm region.
Secondly, the complex geometry of plants had to be considered and its influence on spectral measurements had to be corrected. To do so, we used the model proposed by Vigneau, Ecarnot, Rabatel, & Roumet (2011) to characterize the effects of leaf inclination and specular reflection:

$$R_{meas}\,(\lambda) = \alpha . R_{leaf}\,(\lambda) + \beta$$

where $R_{meas}\,(\lambda)$ and $R_{leaf}\,(\lambda)$ are the measured and actual leaf reflectances respectively. The scalar α models the multiplicative effect caused by leaf inclination ($\alpha = 1$ for leaves perpendicular to the main camera axis), while the scalar β models an additive effect such as specular reflection.
Before calibrating the regression model, several preprocessing steps were therefore implemented to remove the effects of some sources of nuisance variability. First, every spectral pixel was smoothed, thus reducing the spectral noise that was inherent to the image acquisition process. Then, to remove the β influence, every single spectral pixel was mean-centered. In this study, we assumed that the effect of α was negligible, i.e., $\alpha = 1$. Finally, for each HS image, the mean limb spectrum was computed and associated to the measured LNC reference value.

The regression model between the reflectance spectra and LNC measurements was found using PLS regression. The model was calibrated using leave-one-out cross-validation (Naes, Isaksson, Fearn, & Davies, 2002) and the number of latent variables that was needed to best explain the nitrogen variability was obtained by minimizing the root mean square error of cross-validation (RMSECV). The obtained regression model was then applied to individual spectra of HS images and the estimated LNC distribution was evaluated by visual inspection.

3. Results and discussion

3.1. Spectral preprocessing

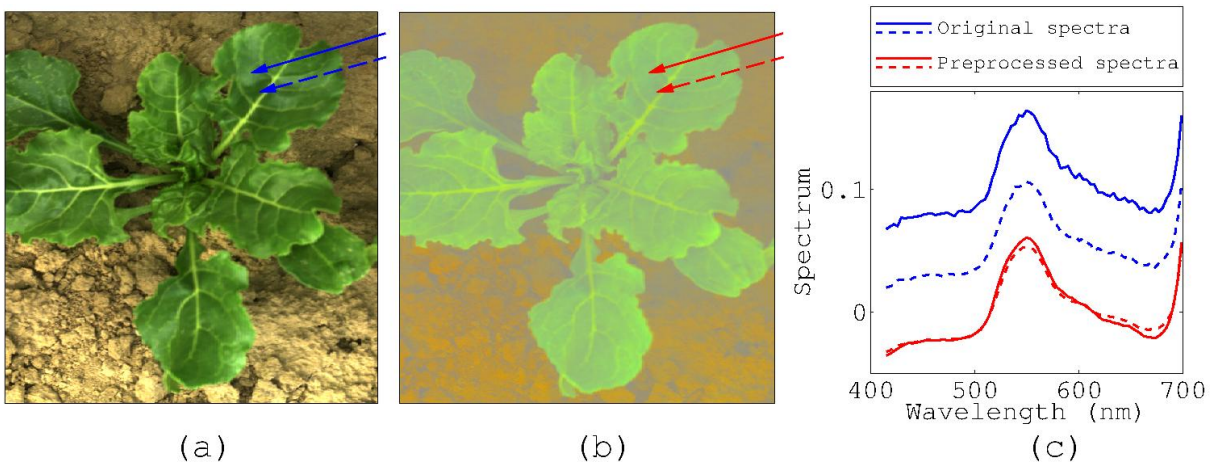

Figure 2: Effect of preprocessing steps : (a) Original true color composite image, (b) False color composite image after preprocessing, and (c) Spectra extracted from regions submitted (dashed lines) or not submitted (solid lines) to specular reflections.

Fig. 2 illustrates the effects of preprocessing steps (i.e., spectral smoothing and constant trend removal) on individual spectra, comparing both the preprocessed HS image and spectra with their original counterpart. The blue arrows in Fig. 2.a (resp. the red arrows in Fig. 2.b) correspond to the blue (resp. red) spectra in Fig. 2.c. Solid (resp. dashed) arrows indicate regions submitted (resp. not submittted) to specular reflections.
Fig. 2.a shows that there were a lot of specular reflections within the whole plant because the sugar beet leaves were waxy. The spectral variability between affected and non-affected regions (highlighted by the blue arrows) that was not correlated with LNC, was greatly reduced after constant trend removal. Indeed, the leaf color distribution of the preprocessed image observed in Fig. 2.b was much more homogeneous than the original one, and the two red highlighted spectra were nearly equal, thus proving the benefits of preprocessing.

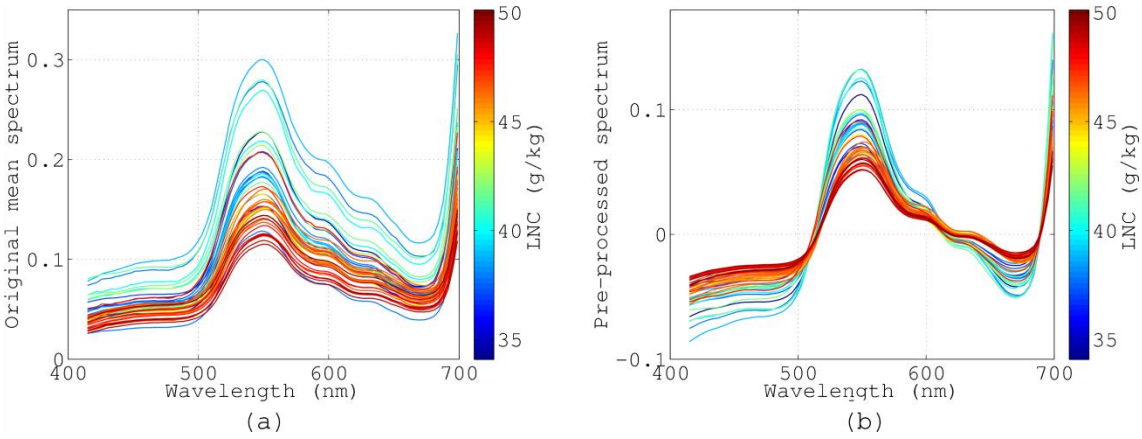

Figure 3: Spectra represented as a function of their LNC value (in g/kg): (a) Original mean spectra, and (b) Preprocessed mean spectra.

For every HS image, preprocessed spectra were then averaged, thus leading to a single mean spectrum. Fig. 3.b shows the obtained mean preprocessed spectra while Fig. 3.a. displays the mean spectra without preprocessing. Even if these are somewhat affected by environmental effects, their global behavior remain the same. For both figures, the color of each spectrum indicates its LNC value (in g/kg).

In general, one sees that the higher the LNC, the more attenuated the reflectance spectra. Indeed, high nitrogen concentrations increase the leaf absorption, thus lowering its reflective power. The two regions where the attenuation was the strongest (410-500 nm and 630-680 nm) corresponded to the absorption features of chlorophyll-a and chlorophyll-b mentioned in Section 2.2 (note that carotenoids also greatly affected the spectra at around 500 nm). As both types of chlorophyll are assumed to be correlated with LNC, the latter can be potentially retrieved using these absorption features.

3.2. PLS modeling

Fig. 4 shows the obtained prediction results. As observed in Fig. 4.a, six latent variables were needed to explain the maximum LNC variability. Using the so-built regression model, LNC was accurately predicted with low RMSECV and high R^2 (RMSECV = 1.72 g/kg; R^2 = 0.86), which indicates that there exists a strong relationship between the mean reflectance spectra and LNC in the 400-700 nm range. Furthermore, when studying each variety separately, one sees that the model led to variable prediction performance depending on the considered variety. LNC was better retrieved in Python plants (RMSECV = 1.59 g/kg; R^2 = 0.90) than in Eleonora plants (RMSECV = 1.87 g/kg; R^2 = 0.80). Such differences can be caused either directly by the plant biochemical properties or indirectly by the plant architecture. In the first case, this would mean that the inner relationship between LNC and reflectance depends on the variety. In the second case, the observed differences between the two varieties would come from measurement errors caused by the plant structure. Indeed, Eleonora plants are more vertical than Python plants, therefore increasing the (uncorrected) effects of leaf inclination and multiple reflections.

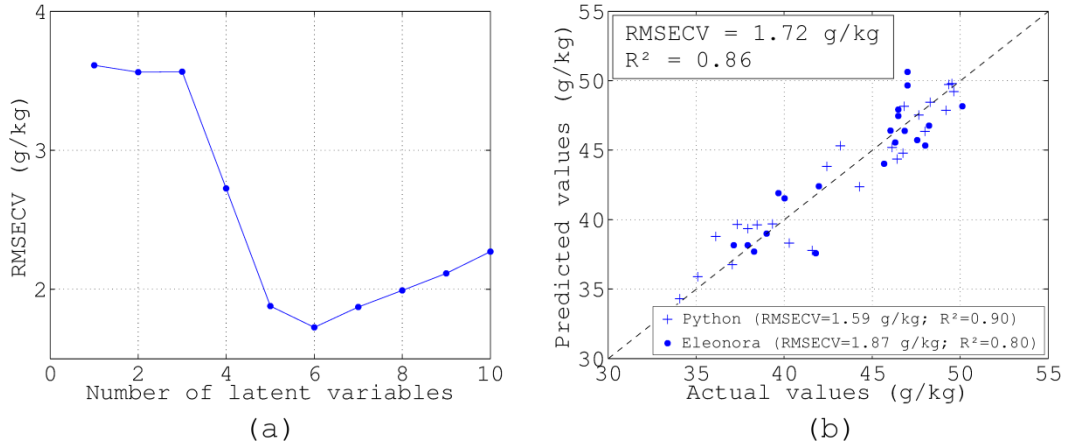

Figure 4: Regression model obtained with the two varieties: (a) RMSECV versus the number of latent variables, and (b) LNC predicted values versus LNC actual values (six latent variables).

3.3. LNC mapping

A strong relationship between reflectance spectrum and LNC was thus established, so we applied the regression model to individual spectra of HS image in order to map the LNC distribution in the whole plants.

The imaged plants had to meet two criteria. First, the nitrogen supply had to be low in order to notice LNC gradients according to leaf age (Hikosaka, Terashima, & Katoh, 1994). Second, the leaves had to be as horizontal as possible to avoid to some extent effects related to leaf inclination and heterogeneous lighting conditions. The true color composite image built from the selected HS image is displayed in Fig. 5.a and the resulting LNC map is displayed in Fig. 5.b (masking out non-vegetation pixels). In the following, the pixel located at line X and column Y is the pixel (X,Y).

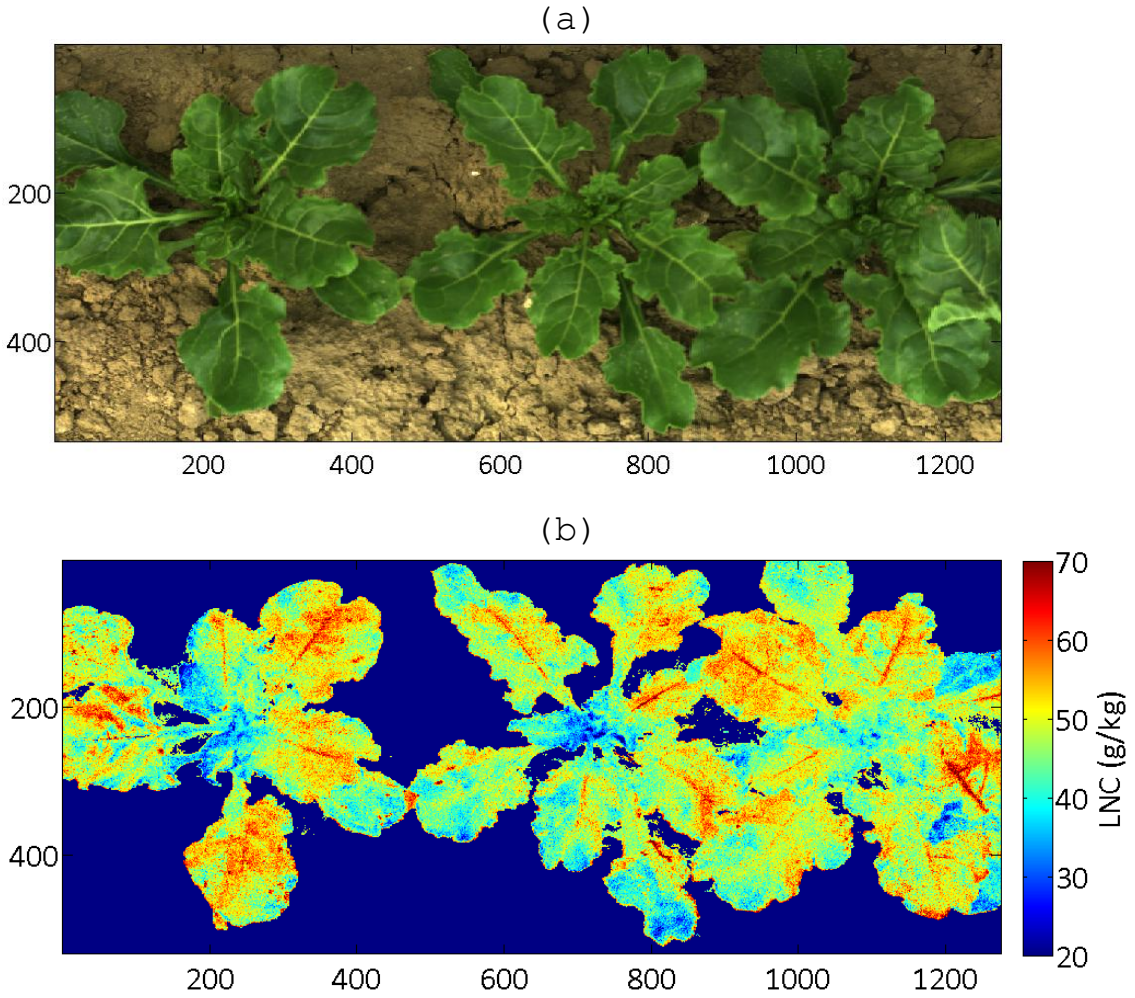

Figure 5: (a) True color composite image, and (b) Estimated LNC map.

First, one sees that specular reflections were well corrected since they did not affect much the estimated LNC spatial distribution. For example, LNC was homogeneous within the leaf centered on pixel (150,950) even though there were strong specular reflections. Furthermore, assuming that the effects of leaf inclination was negligible was reasonable since no particular difference between flattest and steepest leaves was noticed.

Concerning the LNC spatial distribution, the predicted mean value (i.e., 47.50 g/kg) was close to the actual one (i.e., 46.82 g/kg), even though pixels affected by environmental effects (non-homogeneous lighting, multiple reflections) were included in the sample average.

As expected, unlike for high nitrogen supply (data not shown), the obtained LNC distribution was heterogeneous and depended on leaf age. Low LNC values were found in the oldest leaves, e.g., those centered on pixels (150,1240), (500,800) or (40,550). Indeed, such leaves are located at the base of the plants and therefore submitted to a low light level. Moreover, they are first affected in case of nitrogen deficiency. Chloroplasts (containing chlorophyll) degrade and nitrogen is translocated to younger leaves (Lemaire, Onillon, Gosse, Chartier, & Allirand, 1991). Such a transformation reveals underlying carotenoid pigments that were masked by chlorophyll, thus giving senescent leaves a yellow tone (e.g., see pixel (150,1240)).

On the other hand, high LNC values were retrieved in the widest young leaves, e.g., those centered on pixels (100,350), (150,950) or (300,1250). Typically, these leaves are well exposed to sunlight, which increases the number of chloroplasts and stimulates photosynthetic activity. Because the latter is related to LNC (Evans, 1983), these results were therefore consistent.

However, some of the youngest leaves located at the centers of the plants (e.g., those centered on pixels (170,190), (280,200) or (250,670)) were found to have low LNC values, while such zones are usually nitrogen-rich (Gastal & Nelson, 1994). A possible reason for this result is that such zones do not contain as many chloroplasts as mature leaves. Because the obtained indirect relationship between reflectance spectrum and LNC was especially based upon the usual positive correlation between LNC and chlorophyll content (Evans, 1983), no correlation implies bad LNC prediction results. In addition to these physiological considerations, such incongruencies may also be due to nitrogen deficiency or the above mentioned environmental effects that were more influential in these zones.
Lastly, it is worth noting that the LNC values predicted in veins were depending on leaf age. In most cases, LNC was high in the veins located in young leaves while no difference between limbs and veins was observed in old leaves. As veins are responsible for nitrogen transportation from the root to the shoot, this may show how the nitrogen translocation process was occurring when the HS image was acquired. Indeed, because the considered plants were nitrogen-deficient, this nutrient was primarily translocated to younger leaves, therefore explaining this heterogeneity.

4. Conclusions

In this study, we investigated the potential of close-range hyperspectral imaging for LNC retrieval in sugar beet under in-field conditions. To do so, two varieties subjected to four different nitrogen applications were imaged at two growth stages. For every replicated row, about five plants were imaged and sent to the laboratory for measuring the average LNC.
Before using such images, several preprocessing steps were applied to image individual spectra in order to remove some sources of variability that were uncorrelated to LNC, i.e., specular reflections and spectral noise. Then, PLS regression was used to calibrate a regression model between mean reflectance spectra and LNC. With six latent variables, a strong relationship was obtained with high R^2 and low error (RMSECV = 1.72 g/kg; R^2 = 0.86).
Applying the regression model to individual spectra of an HS image led to a consistent LNC map of imaged plants. This map shows both how nitrogen accumulates in leaves and how it is transported within plants. Low LNC values were found in old nitrogen-deficient leaves, while high LNC values were retrieved in young wide leaves. As LNC estimation was based on its correlation with chlorophyll, some incongruencies were observed when there was no correlation, i.e., in the few youngest leaves.
To avoid such problems and allow a direct LNC retrieval, it would be interesting to consider a wider spectral range containing the nitrogen absorption peaks (situated between 1500 nm and 2500 nm).

5. Acknowledgements

This study was funded by the French National Research Agency, within the program ”Investissements d’avenir” with the reference ANR-11-BTBR-0007 (AKER project). We are grateful to the French Sugar Beet Technical Institute (ITB), which made the Becam platform available to us and carried out LNC measurements within AKER project.

6. References

Curran, P. (1989). Remote sensing of foliar chemistry. *Remote sensing of environment , 30*, 271-278.

Evans, J. (1983). Nitrogen and photosynthesis in the flag leaf of wheat (Triticum aestivum L.). *Plant Physiology , 72*, 297-302.

Gastal, F., & Nelson, C. (1994). Nitrogen use within the growing leaf blade of tall fescue. *Plant Physiology , 105*, 191-197.

Hikosaka, K., Terashima, I., & Katoh, S. (1994). Effects of leaf age, nitrogen nutrition and photon flux density on the distribution of nitrogen among leaves of a vine (Ipomoea tricolor cav.) grown horizontally to avoid mutual shading of leaves. *Oecologia , 97*, 451-457.

Lemaire, G., Onillon, B., Gosse, G., Chartier, M., & Allirand, J. (1991). Nitrogen distribution within a lucerne canopy during regrowth: relation with light distribution. *Annals of Botany , 68*, 483-488.

Naes, T., Isaksson, T., Fearn, T., & Davies, T. (2002). *A User Friendly Guide to Multivariate Calibration and Classification.* NIR Publications.

Schlemmer, M., Gitelson, A., Schepers, J., Ferguson, R., Peng, Y., Shanahan, J., Rundquist, D. (2013). Remote estimation of nitrogen and chlorophyll contents in maize at leaf and canopy levels. *International Journal of Applied Earth Observation and Geoinformation , 25*, 47-54.

Vigneau, N., Ecarnot, M., Rabatel, G., & Roumet, P. (2011). Potential of field hyperspectral imaging as a non destructive method to assess leaf nitrogen content in wheat. *Field Crops Research , 122*, 25-31.

Wang, W., Yao, X., Yao, X., Tian, Y., Liu, X., Ni, J., et al. (2012). Estimating leaf nitrogen concentration with three-band vegetation. *Field Crops Research , 129*, 90-98.